

# Positron Annihilation Lifetime Measurements of Free Volume in Wholly Aromatic Copolyesters and Blends

C. M. McCullagh,<sup>†</sup> Z. Yu,<sup>‡</sup> A. M. Jamieson,<sup>\*,†</sup> J. Blackwell,<sup>†</sup> and J. D. McGervey<sup>‡</sup>

Departments of Macromolecular Science and Physics, Case Western Reserve University, Cleveland, Ohio 44106-7202

Received March 29, 1995; Revised Manuscript Received June 20, 1995\*

**ABSTRACT:** The temperature dependence of free volume in random copolyesters of hydroxybenzoic acid (HBA) and hydroxynaphthoic acid (HNA) has been studied from  $-50$  to  $+350$  °C by measuring the average lifetime,  $\tau_3$ , and intensity,  $I_3$ , of *ortho*-positronium (*o*-Ps) annihilation. These parameters have also been used to determine the fractional free volume,  $h_{ps}$ . Significant changes in the temperature coefficients of  $\tau_3$ ,  $I_3$ , and  $h_{ps}$  are observed at the  $\alpha$ -transition temperature,  $T_\alpha$ , and at the melt transition temperature,  $T_m$ . The results indicate that both the average size and the number of free volume cavities occupied by positronium increase at  $T_\alpha$ , continue to increase uniformly with temperature up to  $T_m$ , and then level off. A miscible blend of 75/25 and 30/70 copoly(HBA/HNA) with overall monomer ratio 60/40 exhibits a single melt transition well below those of the component copolymers or a random copolymer of the same composition, suggesting that the chains are less ordered in the blend. Comparison of PALS data for these systems indicates that the blend has a larger  $h_{ps}$  below  $T_m$ , which is primarily due to a larger number of cavities accessible to *o*-Ps, and a substantially larger temperature coefficient of  $h_{ps}$  between  $T_\alpha$  and  $T_m$ . In the nematic melt, the free volume of the blend decreases to that of the pure copolyesters, indicating that  $h_{ps}$  in the nematic phase is independent of composition. Compared to other amorphous or semicrystalline polymers, the HBA/HNA copolymers have both fewer detectable free volume cavities and smaller average cavity sizes, presumably due to the "quenched nematic" morphology of the noncrystalline regions.

## Introduction

Positron annihilation lifetime spectroscopy (PALS) has been successfully applied to measure the fractional free volume in a number of amorphous polymers.<sup>1–6</sup> Specifically, experimental results indicate that the mean free volume hole size,  $\langle v_f \rangle$ , and the number density of holes,  $n_f$ , can be determined from the *ortho*-positronium (*o*-Ps) lifetime and intensity measurements, respectively. When the free volume fraction,  $h_f = n_f \langle v_f \rangle$ , is measured as a function of temperature, thermal transitions such as the glass transition are apparent as a discrete change in the thermal expansion coefficient of free volume,  $dh_f/dT$ .

The positron is the antiparticle of the electron, with the same mass and size but opposite charge. In a vacuum, the free positron lifetime is infinite, but in condensed matter there is a finite probability of annihilation by one of three mechanisms. First, a free positron ( $e^+$ ) may annihilate by colliding with an electron, with the emission of 1–3 photons depending on whether the spin of the electron is opposite or parallel to that of the positron, and on whether the electron is free or bound to an atom. The average lifetime of  $e^+$  in condensed matter is  $\tau_2 = 0.34$ – $0.39$  ns. Second, a positron may combine with an electron to form a bound pair called positronium. When the spins are antiparallel, *para*-positronium (*p*-Ps) is formed. Because *p*-Ps self-annihilates, the average lifetime ( $\tau_1 = 0.124$  ns) is the same regardless of whether it exists in vacuum or in condensed matter. Third, *ortho*-positronium (*o*-Ps) may form when a positron and electron with parallel spins combine. This species, which is preferentially trapped in regions of low electron density, decays mainly

by annihilation of the positron with a bound, molecular electron of opposite spin. This is referred to as *o*-Ps pick-off annihilation. The lifetime of *o*-Ps ranges from  $\tau_3 = 142$  ns in vacuum to  $\tau_3 = 1$ – $3$  ns in condensed matter.<sup>1,2</sup> The relative intensities of *p*-Ps, free  $e^+$ , and *o*-Ps annihilation ( $I_1$ ,  $I_2$ , and  $I_3$ , respectively) are postulated to be proportional to the frequency of each process. Quantum mechanics dictates that  $I_1 = 1/3 I_3$  based on the number of available spin states, and the sum of all three components must be unity. Frequently, however, in amorphous polymers the former relation cannot be satisfied. This is usually attributed to the overlap of the distribution of lifetimes and the limited time resolution of PALS.

The mean lifetime of *o*-Ps can be correlated with the radius,  $R$ , of cavities in matter, and the intensity,  $I_3$ , of the *o*-Ps decay component is assumed to be proportional to the number density of these cavities. A widely used empirical relation between cavity radius and *o*-Ps lifetime is<sup>7,8</sup>

$$\tau_3^{-1} = 2[1 - R/R_0 + 0.159 \sin(2\pi R/R_0)] \text{ (ns}^{-1}\text{)} \quad (1)$$

where the boundary layer thickness,  $\Delta R = R_0 - R = 0.1656$  nm, has been determined empirically by fitting eq 1 to *o*-Ps annihilation data for molecular solids of known pore sizes. The fractional free volume,  $h_{ps}$ , measured by *o*-Ps annihilation can be determined<sup>4,8</sup> as

$$h_{ps} = c I_3 \langle v_f \rangle \quad (2)$$

where the spherical cavity volume is computed as  $\langle v_f \rangle = (4/3)\pi R^3$  and  $c$  is a scaling constant which can be obtained empirically from PVT measurements. Thus  $h_{ps}$  is essentially the product of the number density of cavities and the average cavity volume and therefore is equivalent to the fractional free volume measured by

\* To whom correspondence should be addressed.

<sup>†</sup> Department of Macromolecular Science.

<sup>‡</sup> Department of Physics.

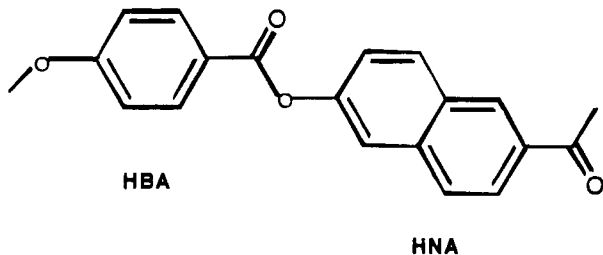
© Abstract published in *Advance ACS Abstracts*, August 1, 1995.

PALS. When PVT data are unavailable, the quantity  $h_{ps}/c$  can be used to qualitatively measure changes in free volume fraction. In these experiments, it is important to note that over the range  $\tau_3 = 1.0$ – $2.0$  ns the cavity size becomes quite small with respect to the boundary layer of electrons and the spherical approximation for  $\langle v_f \rangle$  may become less accurate.

Our previous studies<sup>1,4–6</sup> of *o*-Ps annihilation in amorphous polymers were focused on comparison of  $h_{ps}$  and a theoretical free volume function  $h_{th}$  determined from analysis of PVT data using a statistical mechanical equation of state due to Simha and Somcynsky.<sup>9</sup> Excellent agreement was found between experiment and theory in the melt.<sup>1,4–6</sup> In the glass, significant deviations were observed, in that  $h_{ps}$  became increasingly smaller than  $h_{th}$  as the temperature decreased. More recently,<sup>10</sup> we have found that a conventional free volume quantity, consistent with the theoretical free volume in the melt, accurately describes the *o*-Ps free volume data in both the melt and the glass. This result has provoked a re-examination of the theoretical free volume description in the glass.<sup>11</sup>

PALS has also been applied to study free volume in semicrystalline polymers and blends. Positron annihilation in the semicrystalline polymer poly(aryl ether–ether–ketone) (PEEK) has been studied as a function of the degree of crystallinity,<sup>12</sup> which affects the probability of positronium formation. The degree of crystallinity, as calculated from density measurements, ranged from 0 to 27% in these samples. Although  $\tau_3$  remained constant,  $I_3$  decreased from 22 to 17% as crystallinity increased. Extrapolation of the data indicated  $I_3 = 0$  at 100% crystallinity, suggesting that all positronium formation occurs in the amorphous region. However, the PALS results for poly(ethylene terephthalate) (PET) suggest a small amount of *o*-Ps annihilation is associated with the crystalline fraction ( $I_3 = 0.06$  at 100% crystallinity).<sup>13</sup> Compatible blends of a semicrystalline polyester and amorphous polycarbonate (PC) have also been studied using PALS.<sup>14,15</sup> After subtracting the contributions of the crystalline domains, the authors found that  $\tau_3$  increased and  $I_3$  decreased upon annealing the blends, which was accompanied by an increase in  $T_g$ . They attribute these changes to the effect of increased crystallinity on the amorphous regions, which restricts segmental mobility.

In the present paper, we describe the application of PALS to study the structure of the wholly aromatic random copolyesters prepared from hydroxybenzoic acid (HBA) and hydroxynaphthoic acid (HNA), which have the following structure:



These copolymers have extended chain conformations and form a nematic mesophase above  $T_m$ , which varies from  $\sim 250$  to  $350$  °C depending on the HBA/HNA monomer ratio across the 80/20 to 20/80 composition range.<sup>16</sup> X-ray analysis of the nonperiodic fiber diagrams of these copolyesters has established that these copolymers have a completely random sequence,<sup>17,18</sup> but

nevertheless form ordered structures that give Bragg reflections similar to those for semicrystalline polymers. The degree of crystallinity, as measured by X-ray diffraction, typically ranges from  $\sim 28\%$  in quenched samples to 40–60% after annealing.<sup>19,20</sup> In addition to increasing the degree of crystallinity, thermal annealing also may increase  $T_m$  by altering the chain packing.<sup>20,21</sup> Electron microscopy reveals the formation of crystalline lamellae with dimensions  $\sim 10$  nm along the chain axis and  $\sim 200$  nm laterally<sup>22</sup> after cooling rapidly from the nematic melt. These ordered lamellae are separated by “quenched nematic” regions, where the extended chains are parallel but have more disordered packing. As a result, the densities of the lamellar and interlamellar regions are very similar.  $\Delta H_m$  is relatively small ( $\sim 0.5$ – $0.9$  kJ/mol), indicating that there is little conformational difference between the solid and nematic states,<sup>20</sup> which gives these copolymers their commercial utility for the production of precision moldings.

The HBA/HNA copolyesters show a number of relaxation processes in the solid state, as evidenced by dynamic mechanical<sup>23</sup> and dielectric relaxation studies.<sup>24,25</sup> An  $\alpha$ -transition, similar to a glass transition, is observed at  $\sim 100$  °C for all HBA/HNA copolymers, which shifts to slightly higher temperatures with increasing HNA content. A  $\beta$ -relaxation, which occurs at approximately room temperature, corresponds to the rotation of naphthalene units in the chain. The temperature at which this relaxation occurs depends on composition, increasing as HNA content increases. A weak  $\gamma$ -relaxation is detected at  $\sim -60$  °C, which arises due to the rotation of the phenylene units.

Oriented samples of the HBA/HNA polyesters show anisotropic thermal expansion. Although the radial expansion is positive,<sup>26,27</sup> the expansion in the fiber direction is typically small and negative, on the order of  $-7 \times 10^{-6}$  K<sup>-1</sup> below the  $\alpha$ -transition. Above this temperature, the axial coefficient of thermal expansion decreases rapidly,<sup>28</sup> as increasing thermal motions cause the chains to become more sinuous. However, the mechanical properties do not decrease sharply at the  $\alpha$ -transition, but rather show a gradual decline over a range of temperatures.<sup>23</sup>

We have used PALS to study the changes in free volume that occur as a function of temperature for copoly(HBA/HNA) preparations with three composition ratios. We have also compared the properties of a blend of 30/70 and 75/25 HBA/HNA with those of a random copolyester of the same overall monomer composition. In a previous paper,<sup>29</sup> we have shown that 75/25 and 30/70 HBA/HNA form a compatible blend that exhibits a single broad melt transition at  $T_m = 227$  °C as compared to 288 and 303 °C, respectively, for the components. X-ray analysis showed that the blend undergoes transesterification to a random copolymer of intermediate composition (60/40) upon compression molding at 315 °C. This process is complete after 60 min, during which time  $T_m$  for the blend increases slowly to 248 °C, the melting point of the random copolymer of the same monomer composition. The lower  $T_m$  for the compatible blend probably reflects the greater disorder in the “crystalline” array formed by mixtures of chains with two different comonomer sequence statistics. We have applied PALS to obtain additional insights into the difference in structure and morphology between the compatible blend and transesterified blends. In this study, we attempt to correlate free volume changes with thermal transitions occurring in the HBA/

HNA random copolyesters. We also examine how free volume varies as a function of copolymer composition and upon melt blending two copolymers of different compositions.

## Experimental Section

**Materials and Sample Preparation.** Specimens of 75/25, 30/70, and 58/42 copoly(HBA/HNA) were generously provided by Hoechst Celanese Co., Summit, NJ, in the form of melt-extruded pellets. Fibers of these copolyesters were drawn by hand from the nematic melt on a hot plate. The melt blend of 30/70 and 75/25 copoly(HBA/HNA) was obtained by first weighing pellets of the two copolymers in proportion to give an overall monomer mole ratio of 60/40. The mixture was melted at 310 °C and stirred thoroughly by hand using a metal spatula for 5 min before drawing fibers from the nematic melt. The fibers were then finely chopped and divided into 500 mg portions for compression molding and ~8 mg portions for thermal analysis.

Compression molding of chopped fibers was performed using a Carver Laboratory Press. The platens were preheated to 315 °C after which the sample was inserted and allowed to equilibrate without application of pressure for 10 min. Specimens were subjected to 1800 psi pressure at 315 °C for 3 min and then cooled to room temperature within 20 min. X-ray analysis<sup>29</sup> indicates that transesterification is negligible in the blend during this preparation history. The molded samples were 2 mm thick and were shaved into two disks of diameter 1 cm. To determine the effect of thermal history on free volume, samples of the 75/25 copolymer were prepared as described above and then annealed at either 210 or 275 °C for 24 h under vacuum.

**X-ray and Thermal Analysis.**  $\theta/\theta$  diffractometer scans of unoriented shavings of the compression-molded samples were obtained using a Philips P3100 diffractometer, using a slit width of 0.17°. Scans over  $2\theta = 3\text{--}50^\circ$  were performed at 0.02° increments using 10 s counting intervals. The degree of crystallinity was determined using Gaussian-Lorentzian peak fitting to resolve the crystalline and amorphous peaks. Differential scanning calorimeter (DSC) scans were obtained using a Perkin-Elmer DSC-7. Data were recorded in the temperature range 25–350 °C, with a heating/cooling rate of 20 °C/min. The temperatures of the  $\alpha$ -transition,  $T_\alpha$ , and the solid-nematic transition,  $T_m$ , were determined from the second heating scan.

**Spectroscopic Measurement and Data Analysis.** The positron lifetime spectrometer consisted of a positron source, two  $\gamma$ -ray detectors, a fast-fast coincidence system, and a PC-based multichannel analyzer. The positron lifetime spectra were obtained by determining the time interval between detection of the 1.27 MeV  $\gamma$ -ray which accompanies nuclear decay and the 0.511 MeV  $\gamma$ -ray from the positron annihilation event. The positron source consisted of approximately 1 MBq of <sup>22</sup>Na deposited in an envelope of aluminum foil and sandwiched between two copolyester sample disks. This sandwich was completely enclosed in a copper sample holder, so that good thermal contact to the sample was guaranteed. Heating wires mounted at opposite sites of the sample holder, and two platinum resistance temperature sensors (Model PT-111, Lake Shore Cryogenics) mounted inside the sample holder, were connected to a temperature controller (Model 330, Lake Shore Cryogenics). The sample holder was contained in a vacuum chamber. The temperature was maintained to within  $\pm 0.2$  °C during data acquisition periods (about 1½ h).

Two conical BaF<sub>2</sub> crystals (1.0 × 1.1 × 0.6 in.) were used to detect both the 1.27 MeV  $\gamma$ -ray which served as the positron "birth" signal and the 0.511 MeV annihilation  $\gamma$ -ray. A fast-fast coincidence system based on EG & G Ortec NIM modules (Model 583 constant fraction discriminators and Model 566 time-to-amplitude converter) was employed to correlate voltage pulses from the "birth" and "death"  $\gamma$ -rays. Using <sup>60</sup>Co as a standard, the full width at half-maximum of the time resolution of the system was about 180 ps. Positron lifetime spectra with more than 1.2 million counts were collected using a

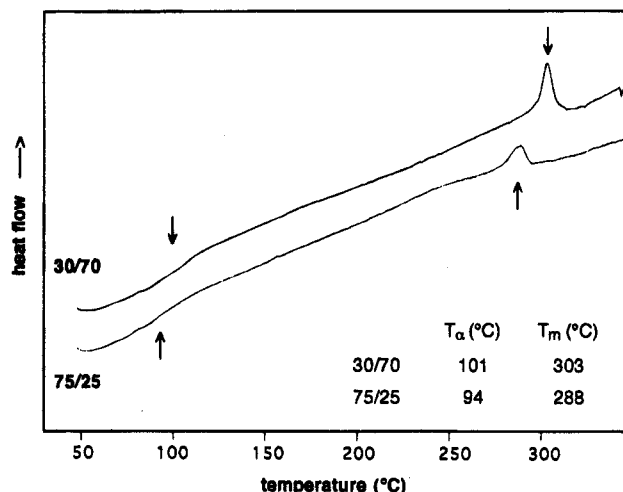


**Figure 1.** DSC scans of the 30/70 (upper curve) and 75/25 (lower curve) HBA/HNA copolymers (second heating scan).  $T_\alpha$  and  $T_m$  are indicated with arrows.

multichannel analyzer (PCA-II, The Nucleus Inc.) installed in a 386 PC.

Data were collected sequentially at temperatures between -50 and +350 °C at ~20 deg increments. The samples were allowed to equilibrate at the specified temperature for 15 min before measurement. Repeated experiments on the 75/25 copolymers showed negligible decreases in *o*-Ps intensity due to prolonged exposure to  $e^+$  radiation, indicating that a buildup of positive charge in the sample (which would result in a reduction in  $I_3$  with increasing exposure time) was minimal under the test conditions described.<sup>30</sup>

The program PATFIT-88<sup>31</sup> was employed to determine positron annihilation lifetimes and intensities. A two-component source correction term was assumed to account for annihilation occurring in the source and in the foil.<sup>5</sup> The time resolution function of the spectrometer was constructed by fitting to a Gaussian function. The positron annihilation spectra were fitted to three exponentially decaying lifetime components: *p*-Ps, free positron, and *o*-Ps. The *p*-Ps lifetime  $\tau_1$  was constrained to the theoretical value of 120 ps,<sup>5</sup> and the sum of the intensities to be equal to 100%.

## Results

**HBA/HNA Copolymers and Blends.** DSC scans of 75/25 and 30/70 copoly(HBA/HNA) are shown in Figure 1. The copolymers each exhibit an  $\alpha$ -transition at ~100 °C and a melt transition at 288 and 303 °C for the 75/25 and 30/70 compositions, respectively. As determined previously,<sup>29</sup> the 58/42 copolymer has a melt transition at 248 °C, and that of the unreacted 1:2 blend of 30/70 and 75/25 HBA/HNA occurs at 227 °C.

Positron annihilation spectra for the 75/25 HBA/HNA copolymer at 50 and 290 °C are shown in Figure 2 as examples of the data collected below and above  $T_\alpha$ , respectively. Each spectrum is composed of three exponential decay functions corresponding to the three mechanisms of positron annihilation. The component with the longest mean lifetime,  $\tau_3$ , is that for *o*-Ps annihilation, which is sensitive to changes in free volume in the sample. This is apparent in Figure 2, in which we observe a large increase in the amplitude of the longest-lived *o*-Ps component at the higher temperature (Figure 2b). This is direct evidence that an increase in temperature increases the number of the cavities sampled by *o*-Ps in the copolymer.

After resolution of the PALS spectra for the 75/25 HBA/HNA copolymer into three decay components using PATFIT-88,  $\tau_3$  and  $I_3$  were plotted as a function of temperature, as shown in Figure 3a,b. The average

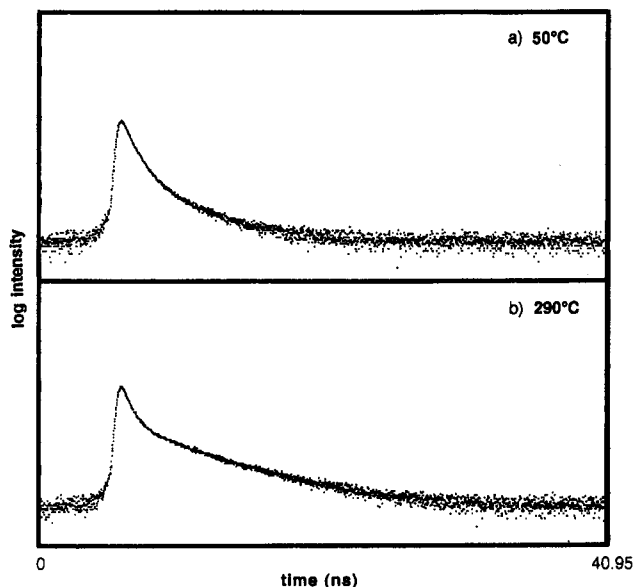


**Figure 2.** Positron annihilation spectra for 75/25 HBA/HNA at (a) 50 °C and (b) 290 °C.

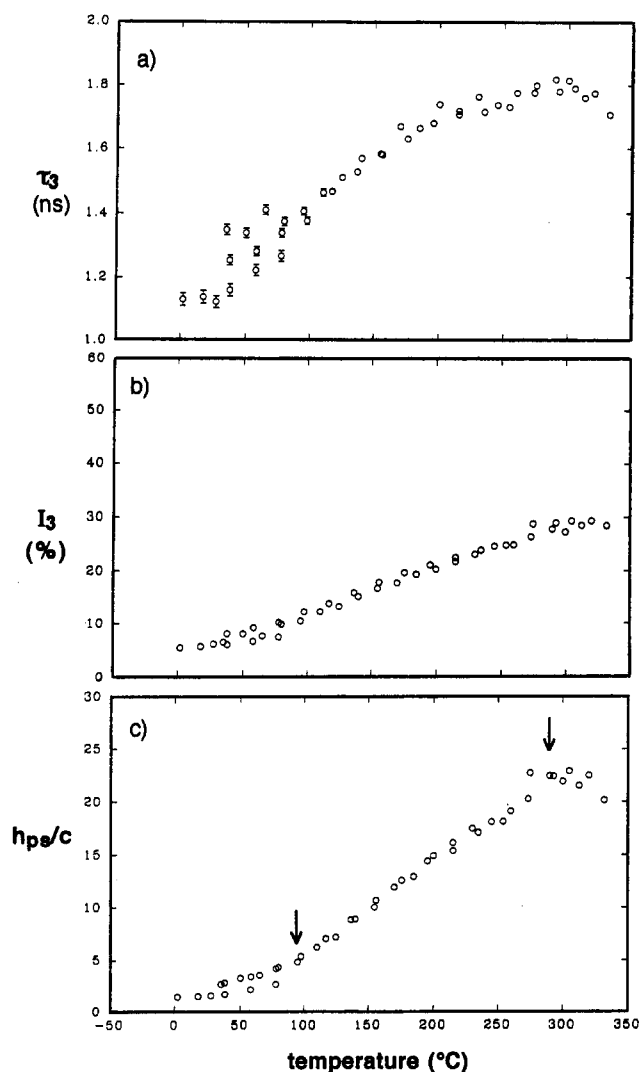


**Figure 3.** PALS data for 75/25 HBA/HNA as a function of temperature: (a) average *o*-Ps lifetime ( $\tau_3$ ), (b) intensity ( $I_3$ ), and (c) free volume fraction ( $h_{ps}/c$ ) as a function of temperature.  $T_\alpha$  and  $T_m$  are indicated with arrows.

*o*-Ps lifetime increased substantially from ~1.1 to 1.8 ns as the temperature was raised from 0 to ~330 °C.

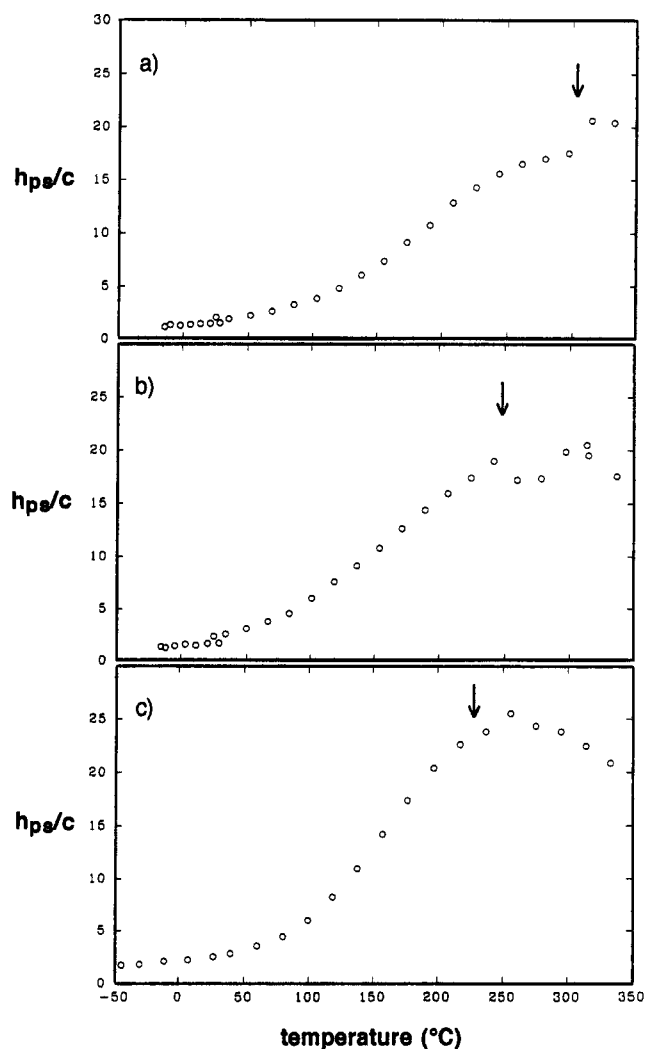


**Figure 4.** Free volume fraction as a function of temperature for (a) 30/70, (b) 58/42, and (c) a blend of 30/70 and 75/25 HBA/HNA.  $T_m$  is indicated with an arrow.

The data shown are for three samples of 75/25 HBA/HNA, and although the experimental error for a given sample is quite small, fluctuations in  $\tau_3$  below 100 °C are observed between samples. This is due to the extremely small values of both  $\tau_3$  and  $I_3$  in this temperature range, which decrease the accuracy of the measurement. The *o*-Ps intensity also increased from 5 to 30% over this temperature interval. Together, this indicates a substantial increase in both the size and the number of cavities which can be detected by this method. The corresponding increase in the fractional free volume ( $h_{ps}/c$ ) with temperature (eq 2) is shown in Figure 3c. The  $\alpha$ -transition (~100 °C) and the melt transition (288 °C), as measured by DSC, correlate quite closely with changes in the slope of  $h_{ps}/c$  as a function of temperature. This change in  $I_3$  by a factor of ~6 is very interesting, as most systems studied by PALS show a much smaller temperature dependence of  $I_3$  in the absence of any phase changes. Such large changes have only been seen previously as discontinuities where a melting transition occurs.

Plots of the *o*-Ps fractional free volume versus temperature for the 30/70 and 58/42 copolymers, and the 1:2 melt blend of 30/70 and 75/25 HBA/HNA are shown in Figure 4. Qualitatively, the temperature dependence of  $h_{ps}/c$  is in each case quite similar to that of the 75/25 copolymer. The  $\alpha$ -transition of each copolymer is manifested as a change in slope of  $h_{ps}/c$  at ~100 °C. The melt

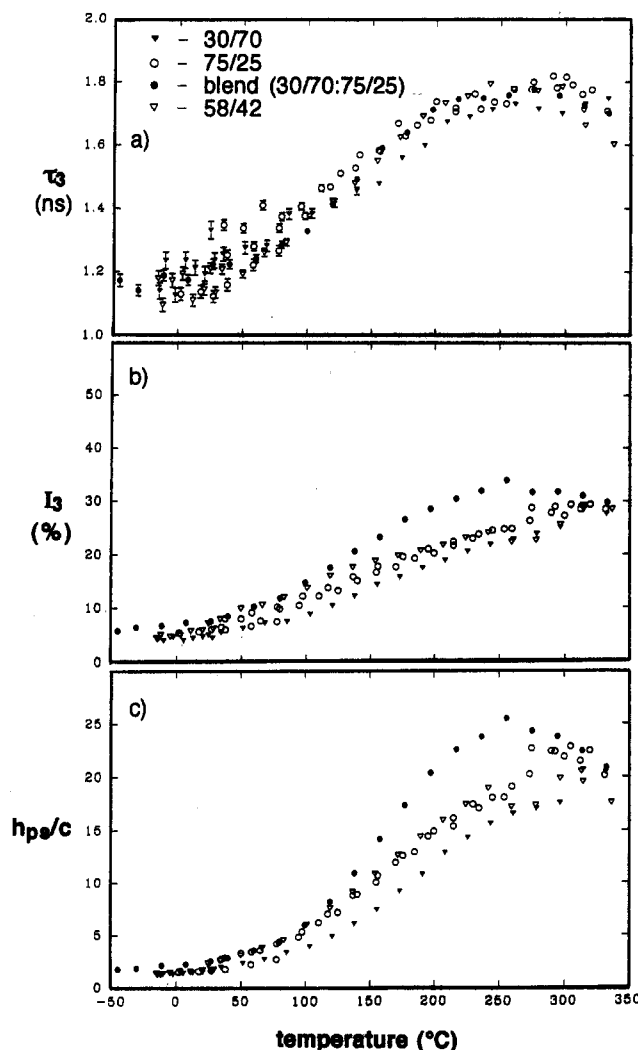


**Figure 5.** Comparison of PALS data for 30/70, 58/42, and 75/25 HBA/HNA and a blend of 30/70 and 75/25 HBA/HNA: (a) average o-Ps lifetime, (b) o-Ps intensity, and (c) free volume fraction as a function of temperature.

transitions at 303 and 248 °C for the 30/70 and 58/42 copolymers, respectively, are also evident as changes in the temperature coefficient of o-Ps free volume. The apparent  $T_m$  of the blend from o-Ps annihilation measurements ( $\sim 250$  °C) is higher than that measured by DSC (227 °C), which may be due to the accumulated annealing which accompanies the positron annihilation measurements. Annealing is known to increase the observed melt transition of the HBA/HNA copolymers and their blends,<sup>20,21,29</sup> but this effect may not be observed in samples which have a single composition because they have better initial packing and therefore require longer annealing times before significant shifts in  $T_m$  are detected. It is also possible that transesterification has occurred in the melt blend, which would again result in a higher melt transition.<sup>29</sup>

Figure 5 shows superimposed plots of  $I_3$ ,  $\tau_3$ , and  $h_{ps}/c$  against temperature for the 30/70, 58/42, and 75/25 copolymers and the blend of the 30/70 and 75/25 copolymers. The values of the free volume fraction between the  $\alpha$ -transition and the melt transition are nearly identical for the 75/25 and 58/42 copolymers. However, the o-Ps free volume fraction of the 30/70 copolymer is significantly smaller than that of the other two HBA/HNA compositions studied. The lower values of  $\tau_3$  and  $I_3$  (Figure 5a,b) indicate that the difference in  $h_{ps}$  is due to both smaller cavity size and fewer cavities

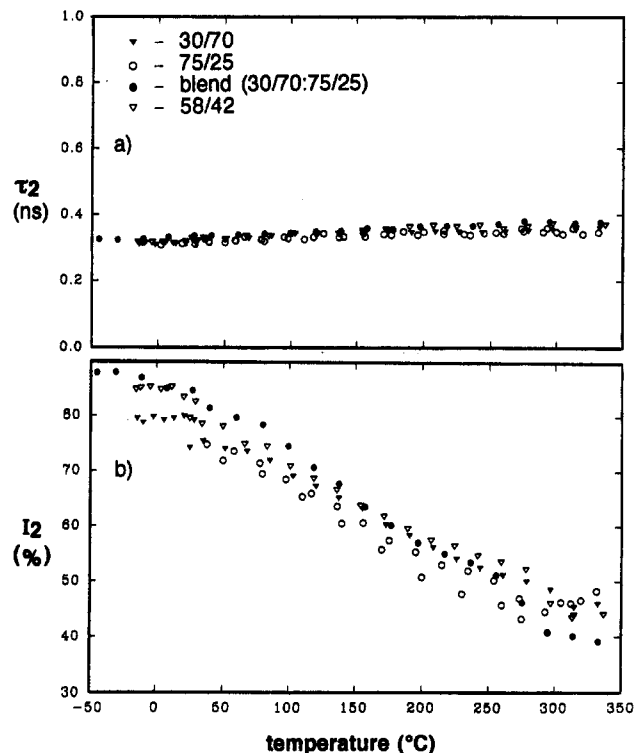


**Figure 6.** (a)  $\tau_2$  and (b)  $I_2$  as a function of temperature for 30/70, 58/42, and 75/25 HBA/HNA copolymers and a blend of 30/70 and 75/25 HBA/HNA.

in the 30/70 copolymer. However, the blend of the 30/70 and 75/25 copolymers has a significantly larger o-Ps free volume in this temperature range (Figure 5c). This arises due to a larger number density of cavities rather than an increased cavity size, as evidenced by an increased  $I_3$  (Figure 5b).

Typically, in amorphous polymers, the fraction of free positron annihilation (measured as  $I_2$ ) remains relatively constant, decreasing slightly to compensate for the increase in  $I_1$  and  $I_3$  with increasing temperature. For the copolymers studied here, however,  $I_2$  is a strongly decreasing function of temperature (Figure 6), whereas  $\tau_2$  increases slightly from 0.34 to 0.39 ns over the temperature range studied. The large decrease in  $I_2$  offsets the unusually large increase in  $I_3$  and smaller increase in  $I_1$ , as shown in Figure 7. As  $I_1$  and  $I_3$  level off above the melt transition,  $I_2$  correspondingly becomes less temperature sensitive as well.

**Effect of Isothermal Annealing.** It has been demonstrated previously that annealing the HBA/HNA copolymers increases the degree of crystallinity and may also alter the chain packing in the crystalline phase.<sup>21,27,34</sup> Annealing below the recrystallization temperature,  $T_c$ , results in an increase in crystallinity while the melt transition and unit cell dimensions are unaffected. Annealing above  $T_c$  results in a partial reordering of the crystalline regions from a pseudohexagonal packing to a more dense orthorhombic form. The melt transition temperature increases by up to 30 deg with increasing annealing time. We examined the effect of annealing the 75/25 copolymer ( $T_c \approx 250$  °C) for 24 h at either at 210 or 275 °C. The X-ray diffractometer scan for the unoriented copolymer contains three crystalline peaks at  $d = 4.60$ , 3.31, and 2.08 Å which are resolved by Gaussian-Lorentzian peak-fitting. These correspond to the strongest equatorial, off-equatorial, and meridional intensities, respectively, in the fiber diagram of the pseudohexagonal form of copoly(HBA/HNA) with unit

**Table 1. Comparison of Positron Annihilation Results for PS, PEEK, and the HBA/HNA Copolymers at Room Temperature**

	lifetime (ns)	intensity (%)
PS <sup>10</sup>	$\tau_1 = 0.12$	$I_1 = 0.24$
	$\tau_2 = 0.35$	$I_2 = 0.40$
	$\tau_3 = 2.1$	$I_3 = 0.36$
PEEK <sup>12</sup>	$\tau_1 = 0.12$	$I_1 = 0.24$
	$\tau_2 = 0.41$	$I_2 = 0.52-0.57$
	$\tau_3 = 1.8$	$I_3 = 0.18-0.23$
75/25 HBA/HNA	$\tau_1 = 0.12$	$I_1 = 0.17$
	$\tau_2 = 0.31$	$I_2 = 0.75$
	$\tau_3 = 1.2$	$I_3 = 0.08$

cell dimensions  $a = 9.2 \text{ \AA}$  and  $b = 5.3 \text{ \AA}$ .<sup>34</sup> An amorphous peak is also resolved at  $d = 4.52 \text{ \AA}$ . Based on the resolution of these data into components due to the crystalline and amorphous fractions, the percentage crystallinity for the unannealed sample of 75/25 copoly-(HBA/HNA) is  $\sim 28\%$ . Upon annealing at  $210^\circ\text{C}$  for 24 h, the equatorial peak shifts to  $d = 4.50 \text{ \AA}$ . This can be attributed to the development of slightly better chain packing due to better packing of the monomers within the pseudohexagonal form. Using the same peak fitting program to resolve the crystalline and amorphous peaks, the crystallinity of the sample annealed at  $210^\circ\text{C}$  is  $\sim 39\%$ . Annealing the 75/25 copolymer for 30 days at  $275^\circ\text{C}$  results in partial molecular rearrangement into a more dense orthorhombic form with dimensions  $a = 7.1$  and  $b = 5.7 \text{ \AA}$ .<sup>34</sup> After the specimen has been maintained at  $275^\circ\text{C}$  for 24 h the diffractometer scan reveals additional crystalline peaks which correspond to the more dense crystalline form. Thus, both crystalline forms appear to be present in this sample, and the approximate crystallinity is  $\sim 32\%$ .

The fractional free volume was determined for each of these samples by PALS. The values of  $h_{ps}/c$  for the annealed samples were slightly lower than that of the unannealed copolymer in both cases. The sample annealed at  $210^\circ\text{C}$  showed  $\sim 3\%$  reduction in free volume, and the sample annealed at  $275^\circ\text{C}$  exhibited  $h_{ps}/c$  values  $\sim 7\%$  lower than the unannealed sample. These differences originate in a small decrease in cavity size ( $\tau_3$ ), while the number of cavities remains constant or increases slightly. However, these measurements are not significantly different within experimental error. Thus, in contrast to the results reported for semicrystalline polymers,<sup>12,13</sup> the degree of crystallinity in the HBA/HNA copolymers does not appear to have a significant effect on the measured free volume. This can perhaps be attributed to the relatively high degree of order in the noncrystalline interlamellar regions of the HBA/HNA copolymers, which are a quenched nematic phase and are not greatly altered by increasing crystallinity.

## Discussion

Positron annihilation spectroscopy has been previously used to determine changes in free volume in glassy polymers both above and below  $T_g$ . However, in highly crystalline materials, *o*-Ps formation is rare and the primary mode of positron decay is via free positron annihilation.<sup>12</sup> For semicrystalline materials, it is unclear at this time whether we are sampling the free volume associated with the crystalline or amorphous regions, or some combination of these two. As an illustration, Table 1 compares the measured lifetimes and intensities obtained at room temperature for polystyrene (PS), a glassy polymer previously investigated

in this laboratory,<sup>10</sup> and for PEEK, a semicrystalline copolymer,<sup>12</sup> with our present data for 75/25 copoly-(HBA/HNA). The range of values reported for PEEK indicate measurements performed at varying degrees of crystallinity. The largest differences between 75/25 copoly(HBA/HNA) and the other polymers occur in the value of  $\tau_3$ , which is much smaller for the 75/25 copolymer. Even at temperatures as high as  $330^\circ\text{C}$ ,  $\tau_3$  only reaches a value of  $\sim 1.8 \text{ ns}$ , whereas  $\tau_3 \approx 2.5 \text{ ns}$  at  $130^\circ\text{C}$  for PS. This indicates that the cavities are much smaller in the semirigid HBA/HNA copolymer. Another difference occurs in the amplitude of the increase of  $I_3$  with temperature, which is much larger for the HBA/HNA copolymers than for PS. At low temperatures ( $T < T_\alpha \sim 100^\circ\text{C}$ ), the number density of holes as measured by the *o*-Ps intensity in copoly(HBA/HNA) is very small ( $I_3 \sim 0.08$ ), but above this temperature the *o*-Ps intensity increases rapidly to  $I_3 \sim 0.30$  at  $T = 290^\circ\text{C}$ . This is in direct contrast to the results for PS, in which the *o*-Ps intensity remains fairly constant at  $I_3 = 0.35-0.37$  as temperature is increased.

It is clear that in the "semicrystalline" HBA/HNA copolyesters, the free volume fraction measured by *o*-Ps annihilation is consistent with the known temperature dependence of the material properties of these polymers. Specifically, the activation of molecular motion at  $T_\alpha$  coincides with a sudden increase in  $h_{ps}$ , and the transition at  $T_m$  to a nematic melt correlates with a discontinuity and possible leveling off in  $h_{ps}$ . In addition, between  $T_\alpha$  and  $T_m$ , there is a substantial deterioration in the mechanical properties.<sup>23</sup> The tensile modulus steadily decreases with increasing temperature, and its magnitude is independent of composition. It is interesting to note that the tensile modulus of the crystal, measured from the change in X-ray diffraction maxima under tensile strain, exhibits a sharp decrease at  $T_\alpha$ .<sup>28</sup> This arises from an increase in chain sinuosity, which reduces the axial length of the chain while increasing the radial dimensions. This anisotropic expansion may result in a larger  $h_{ps}$  in two ways; first, the increasing chain sinuosity may in itself create new free volume cavities as the temperature is increased, and second, this type of expansion may transform elongated needle-like cavities into more spherical forms. Although the latter process would not alter free volume, the change in cavity shape would result in a larger value for  $\tau_3$  and lead to an apparent increase in hole size.

Another unusual feature of this system is the large value of  $I_2$  at low temperatures, which decreases significantly as the temperature is increased. Because of the high density of the HBA/HNA copolymers, it is possible that  $I_2$  also includes contributions from short *o*-Ps lifetimes which are not included in  $I_3$  at low temperatures, but which become longer as temperature is increased, and hence become incorporated into  $I_3$ . However,  $\tau_2 \sim 0.34 \text{ ns}$  is too small to be due to *o*-Ps annihilation, making this explanation unlikely. It is also possible that the large value of  $I_2$  is due to the annihilation of free positrons in the crystalline regions of the copolymer, as proposed previously.<sup>32</sup> As molecular motions increase above  $T_\alpha$ , the crystalline regions may become more disordered and develop more free volume cavities, thereby decreasing  $I_2$  and increasing  $I_3$ . The most likely explanation, however, is that at low temperatures the free volume cavity sizes are often too small to allow *o*-Ps formation. The radius of *o*-Ps is approximately that of hydrogen,  $R_{o-Ps} = 0.528 \text{ \AA}$ . Using a finite spherical potential well model, a theoretical

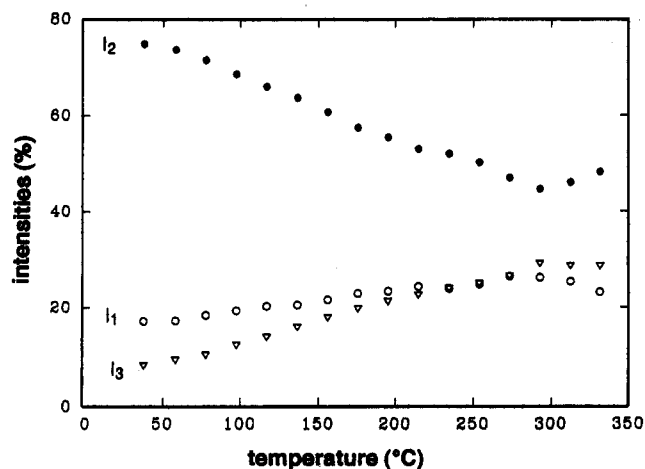


**Figure 7.**  $I_1$ ,  $I_2$ , and  $I_3$  as a function of temperature for 75/25 HBA/HNA.

**Table 2.** Calculation of  $T_\alpha$  and  $d(h_{ps}/c)/dT$  from Fractional Free Volume

HBA/HNA	$T_\alpha$ (°C)	$d(h_{ps}/c)/dT$ (°C <sup>-1</sup> )
30/70	100 ± 3	0.096 ± 0.005
58/42	64	0.096
75/25	65	0.096
blend	84	0.160

analysis suggests that the minimum hole radius capable of being sampled by *o*-Ps is  $R \sim 1.85$  Å.<sup>33</sup> If the free volume cavities have smaller radii than this, they will not be detected by *o*-Ps annihilation, thereby reducing  $I_3$  relative to  $I_2$ . As the temperature increases, the material expands and the cavities increase in size and/or become more spherical in shape, as noted above. More of the previously undetectable holes can be sampled by *o*-Ps, leading to an increase in  $I_3$  (accompanied by a corresponding decrease in  $I_2$ ), as seen in Figure 7, and an increase in  $\tau_3$ .

Although the 75/25 and 58/42 copolymers have similar fractional free volumes in the temperature range studied, the 30/70 copolymer has a smaller fractional free volume, mainly due to a decreased number of cavities. However, the temperature coefficient of  $h_{ps}/c$  is identical for all three copolymers (Table 2). The difference in number of cavities can be explained by the fact that  $T_\alpha$  estimated from the positron data, as reported in Table 2, is significantly larger for the 30/70 copolymer. If the *o*-Ps free volume values are plotted against  $T - T_\alpha$ , the temperature dependence of  $h_{ps}/c$  is identical for the HBA/HNA copolymers regardless of composition. The exact position of  $T_\alpha$  depends on copolymer composition and thermal history<sup>23,35,36</sup> and may be larger for the 30/70 copolymer due to both its larger HNA content and higher melt transition temperature. All samples were compression molded at 315 °C, but this temperature is much closer to the melt transition for the 30/70 copolymer ( $T_m = 303$  °C) than for the 75/25 ( $T_m = 288$  °C) or 58/42 ( $T_m = 248$  °C) copolymers. Incomplete melting of the crystalline domains at this temperature, as noted previously,<sup>37</sup> could explain the elevated  $T_\alpha$  observed for the 30/70 copolymer by placing greater constraints on the mobility of the noncrystalline regions. It is also possible that the greater proportion of HBA in the 75/25 and 58/42 copolymers, which has more rotational mobility than HNA, results in a slightly larger free volume in these polymers. Gas transport studies, for example, indicate that the permeability coefficient for the HBA/HNA copolymers increases with increasing HBA content.<sup>36</sup>

Even after accounting for the shift in  $T_\alpha$ , the fractional free volume is larger and increases more rapidly above  $T_\alpha$  in the blend of 30/70 and 75/25 HBA/HNA (Table 2) than in either blend component or in the random copolymer of approximately the same composition. The increased free volume in the blend suggests there is poorer packing between random copolymers of different compositions and is consistent with the observation that the  $T_m$  of the blend is lower than that of the random copolymer of equal overall composition.<sup>29</sup> A reduction in  $T_m$  has been reported by other investigators for blends of HBA/HNA copolymers of different compositions.<sup>38</sup> Therefore we deduce that melt blending random copolymers further reduces the 3-dimensional order, which may account for the larger number of cavities and increased cavity size detected by PALS in the blend.

The effect of annealing on free volume in 75/25 HBA/HNA is negligible, as determined by PALS. However, we note that the percentage crystallinity increases only slightly upon annealing (from 28% to 32–39%, depending on annealing temperature). Additionally, the rigidity of the polymer chains confines the majority of noncrystalline regions to a "frozen nematic" organization of extended chains.<sup>22</sup> Large changes in *o*-Ps lifetime or intensity due to additional constraints on the noncrystalline regions by the crystalline domains are not likely under these conditions. The observation that the free volume does not increase upon annealing is further consistent with measurements of the bulk density, which does not change appreciably in these materials as a function of thermal history. Studies of the 73/27 copolymer indicate that annealing at 240 °C for 24 h increases the density by ~0.3%, from 1.400 to 1.404 g/cm<sup>3</sup>, while the percentage crystallinity increases by ~13%.<sup>35</sup> The same study also found that the permeability of annealed films decreased for gases with kinetic diameters between 2.60 and 3.64 Å, with the most significant changes occurring for the largest gas molecules. The reduction in permeability for the smallest gas molecule (He) was ~8%. Our results, which indicate a slight reduction in fractional free volume due to smaller cavity sizes, are consistent with these previous findings.

**Acknowledgment.** This work was supported by NSF MRG No. 91-22227 and by the BP America-CWRU Partners in Polymer Science program. We are indebted to Dr. M. Jaffe of Hoechst-Celanese for supplying the polymer specimens.

## References and Notes

- McGervey, J. D.; Walters, V. F. *Phys. Rev. Lett.* **1964**, *13*, 408.
- Schrader, D. M.; Jean, Y. C. *Positron and Positronium Chemistry*; Elsevier: New York, 1988.
- McGervey, J. D.; Panigrahi, N.; Simha, R.; Jamieson, A. M. In *Proceedings of the 7th International Conference on Positron Annihilation*, New Delhi; Jain, P. C., Singru, R. M., Gopinath, K. P., Eds.; World Scientific Publishing: Singapore, 1985; p 822.
- Kobayashi, Y.; Zheng, W.; Meyer, E. F.; McGervey, J. D.; Jamieson, A. M.; Simha, R. *Macromolecules* **1989**, *22*, 2302.
- Kluin, J.-E.; Yu, Z.; Vleeshowers, S. S.; McGervey, J. D.; Jamieson, A. M.; Simha, R. *Macromolecules* **1992**, *25*, 5089.
- Kluin, J.-E.; Yu, Z.; McGervey, J. D.; Jamieson, A. M.; Simha, R.; Sommer, K. *Macromolecules* **1993**, *26*, 1853.
- Tao, S. J. *J. Chem. Phys.* **1972**, *56*, 5499.
- Nakanishi, H.; Wang, S. J.; Jean, Y. C. In *Proceedings of the International Conference on Positron Annihilation in Fluids*, Arlington, TX; Sharma, S. C., ed.; World Scientific Publishing: Singapore, 1987.
- Simha, R.; Somcynsky, T. *Macromolecules* **1989**, *2*, 342.



- (10) Yu, Z.; Yahse, U.; McGervey, J. D.; Jamieson, A. M.; Simha, R. *J. Polym. Sci., Polym. Phys.* **1994**, *32*, 2637.
- (11) Carri, G. M.S. Thesis, Case Western Reserve University, 1994.
- (12) Nakanishi, H.; Jean, Y. C. *J. Polym. Sci., Polym. Phys.* **1989**, *27*, 1419.
- (13) Xie, L.; Gidley, D. W.; Hristov, H. A.; Yee, A. F. *Polymer* **1994**, *35*, 14.
- (14) Simon, G. P.; Zipper, M. D.; Hill, A. J. *J. Appl. Polym. Sci.* **1994**, *52*, 1191.
- (15) Zipper, M. D.; Simon, G. P.; Cherry, P.; Hill, A. J. *J. Polym. Sci., Polym. Phys.* **1994**, *32*, 1237.
- (16) Calundann, G. W.; Jaffe, M. Robert A. Welch Conferences on Chemical Research. *Proc. Synth. Polym.* **1982**, 247.
- (17) Blackwell, J.; Biswas, A.; Gutierrez, G. A.; Chivers, R. A. *Faraday Discuss. Chem. Soc.* **1985**, *79*, 73.
- (18) Blackwell, J.; Chivers, R. A.; Gutierrez, G. A.; Biswas, A. J. *Macromol. Sci.-Phys.* **1985**, *B24* (1-4), 39.
- (19) Butzbach, G. D.; Wendorff, J. H.; Zimmerman, H. J. *Polymer* **1986**, *27*, 1337.
- (20) Cheng, S. Z. D. *Macromolecules* **1988**, *21*, 2475.
- (21) Cheng, H.-M. Ph.D. Dissertation, Case Western Reserve University, 1990.
- (22) Hudson, S. D.; Lovinger, A. J. *Polymer* **1993**, *34*, 1123.
- (23) Troughton, M. J.; Davies, G. R.; Ward, I. M. *Polymer* **1989**, *30*, 58.
- (24) Alhaj-Mohammed, M. H.; Davies, G. R.; Abdul Jawad, S.; Ward, I. M. *J. Polym. Sci., Polym. Phys.* **1988**, *26*, 1751.
- (25) Kalika, D. S.; Yoon, D. Y. *Macromolecules* **1991**, *24*, 3404.
- (26) Flores, A.; Ania, F.; Balta Calleja, F. J.; Ward, I. M. *Polymer* **1993**, *34*, 2915.
- (27) Cheng, S. Z. D.; Janimak, J. J.; Zhang, A.; Zhou, Z. *Macromolecules* **1989**, *22*, 4240.
- (28) Green, D. I.; Orchard, G. A. J.; Davies, G. R.; Ward, I. M. *J. Polym. Sci., Polym. Phys.* **1990**, *28*, 2225.
- (29) McCullagh, C. M.; Blackwell, J.; Jamieson, A. M. *Macromolecules* **1994**, *27*, 2996.
- (30) Li, X. S.; Boyce, M. C. *J. Polym. Sci., Polym. Phys.* **1993**, *31*, 869.
- (31) Kiregaard, P.; Pedersen, N. J.; Eldrup, M. Riso National Laboratory, Denmark, 1989.
- (32) McGervey, J. D.; Walters, V. F. *Phys. Rev. B* **1970**, *2*, 2421.
- (33) Yu, Z. Ph.D. Thesis, Case Western Reserve University, 1995.
- (34) Sun, Z.; Cheng, H.-M.; Blackwell, J. *Macromolecules* **1991**, *24*, 4162.
- (35) Weinkauff, D. H.; Paul, D. R. *J. Polym. Sci., Polym. Phys.* **1992**, *30*, 817.
- (36) Weinkauff, D. H.; Paul, D. R. *J. Polym. Sci., Polym. Phys.* **1992**, *30*, 837.
- (37) Gusky, S. M.; Winter, H. H. *J. Rheol.* **1991**, *35* (6), 1991.
- (38) DeMeuse, M. T.; Jaffe, M. *Mol. Cryst. Liq. Cryst.* **1988**, *157*, 535.

MA950441G